Gaugement of the inner space of the Apomyoglobin's heme binding site by a single free diffusing proton

I. Proton in the cavity

E. Shimoni, Y. Tsfadia, E. Nachliel, and M. Gutman

Laser Laboratory for Fast Reactions in Biology, Department of Biochemistry, George S. Wise Faculty of Life Sciences, Tel Aviv University, Ramat Aviv 69978, Israel

ABSTRACT Time resolved fluorimetry was employed to monitor the geminate recombination between proton and excited pyranine anion locked, together with less than 30 water molecules, inside the heme binding site of Apomyoglobin (sperm whale).

The results were analyzed by a numerical reconstruction of the differential rate equation for time-dependent diffusion controlled reaction with radiating boundaries using N. Agmon's procedure (Huppert, Pines, and Agmon, 1990, *J. Opt. Soc. Am. B.*, 7:1541–1550). The analysis of the curve provided the effective dielectric constant of the proton permeable space in the cavity and the diffusion coefficient of the proton.

The electrostatic potential within the cavity was investigated by the equations given by Gilson et al. (1985, *J. Mol. Biol.*, 183:503–516). According to this analysis the dielectric constant of the protein surrounding the site is $\epsilon_{prot} \leq 6.5$.

The diffusion coefficient of the proton in the heme binding site of Apomyoglobin-pyranine complex is $D = 4 \cdot 10^{-5}$ cm^2/s. This value is ~50% of the diffusion coefficient of proton in water. The lower value indicates enhanced ordering of water in the cavity, a finding which is corroborated by a large negative enthropy of binding $\Delta S^0 = -46.6$ cal · mole^{-1} deg^{-1}.

The capacity of a small cavity in a protein to retain a proton had been investigated through the mathematical reconstruction of the dynamics. It has been demonstrated that Coulombic attraction, as large as $\Delta\psi$ of energy coupling membrane, is insufficient to delay a free proton for a time frame comparable to the turnover time of protogenic sites.

INTRODUCTION

Proton transfer across membranes is an established biochemical reaction involved in homeostasis and ATP synthesis. The proteins which carry out this reaction are numerous and some of them, like the F_0-F_1 ATPases or Bacterial Rhodopsin, are extensively studied proteins. Yet the mechanism by which they pump proton is still obscure. The reason for the lack of understanding is a combination of two handicaps: the detailed structure of the proton pumping site is unknown and the process of proton transfer cannot be studied at sufficient time resolution.

Bacterial Rhodopsin, perhaps the most studied proton pump, has been investigated up to the level of identification of the individual groups involved in pumping (Varo and Lanyi, 1990, 1991; Gerwert et al., 1990; Henderson et al., 1990). Yet due to the multiple step process and the sequentiality of the events, each with its time constants, synchronization is rapidly lost. In this manuscript we shall avoid these difficulties by investigating a well defined model system, a pyranine molecule (8 hydroxy pyrene 1,3,6-tri sulfonate) enclosed in the heme binding site of Apomyoglobin (Gutman and Nachliel, 1982). The advantage of this system is the high level of synchronization it can gain. The reaction, photodissociation of the hydroxy proton, is initiated with a ~1 ps laser pulse and the dissociation itself proceeds immediately with typical rate constants corresponding with subnanosecond dynamics. Previous studies (Gutman and Nachliel, 1982) were carried out in a rather short observation window (2 ns). This short observation was insufficient for deriving a precise quantitation of the events. The improvement of the instrumentation (time correlated single photon counting) and a powerful analytical methodology introduced by Agmon and co-workers (Pines, Huppert and Agmon, 1988; Huppert, Pines and Agmon, 1990; Agmon and Szabo, 1991) allowed us to look at the events with high resolution and deduce how the shape and dimension of a site effects the dynamics of a single proton caged in it.

Recently there have been enzymological studies illuminating the role of water molecules which are inside the functional cavity of enzymes (Zimmerberg and Parsegian, 1986; Kornblat and Hao, 1990). These studies implicated that intracavity water molecules are essential for propagation of proton in proton pumping proteins. This point is readily covered by our studies. The analysis of the proton production and propagation in the heme binding site reveals that the water molecules form a matrix differing in properties from bulk water; it exhibits reduced activity (a_{H2O}) and diminished diffusion coefficient (D_{H+}), both compatible with enhanced ordering of the water by the protein.

In this series of studies we investigate in this manuscript, the (sub)nanosecond dynamics of the proton: concentrating on the events associated with the diffusion of the proton inside the site and how it escapes to the bulk against a strong electrostatic attraction. In the following manuscript (Shimoni, Nachliel, and Gutman, 1993) we shall concentrate on the microsecond dynamics of a bulk proton diffusing into the heme binding

Address correspondence to M. Gutman.

0006-3495/93/02/472/08 $2.00

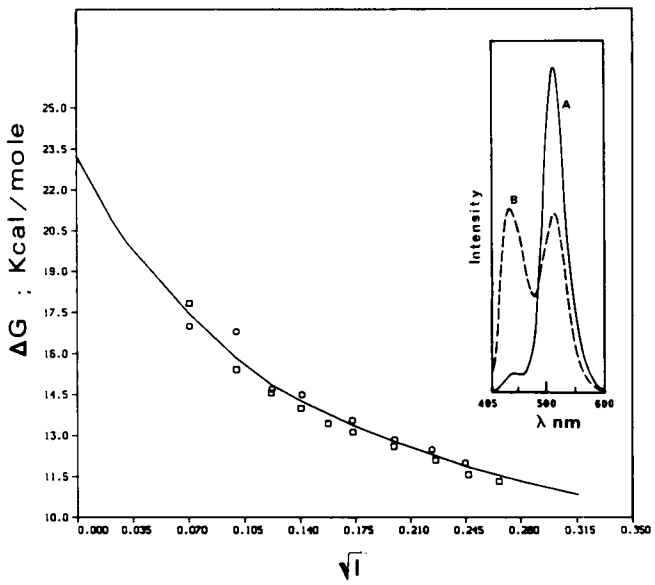

FIGURE 1 The dependence of the binding energy of the dye-protein complex on the ionic strength. The binding constant was calculated from the fluorescence emission curve (see *inset*) according to Gutman and Nachliel (1982). The ionic strength was adjusted by addition of NaCl. The curve drawn in the figure was calculated according to equations 1 and 2 with $Z_{prot} = +11$ and $\Delta G_{other} = 2.5$ Kcal/mol. (*Inset*) The fluorescence emission spectrum of pyranine (3.4 μM) in water (*A*) and in presence of 40 μM Apomyoglobin, all at pH = 5.

pocket of the dye-apoprotein complex. These two manuscripts thus cover the two main aspects of a protogenic site: how it interacts with proton in the bulk and what the fate of the proton is once it gets inside.

MATERIALS AND METHODS

Apomyoglobin was prepared from sperm whale myoglobin (Sigma Chemical Co., St. Louis, MO) by cold acidic ecetone extraction (Antonini and Brunori, 1971); pyranine (8 hydroxy pyrene 1,3,6 tri sulfonate) laser grade was purchased from Kodak.

Steady-state fluorescence was measured by a Shimadzu RF 540 spectrophotometer in a thermostated cell.

Time resolved fluorescence was measured by time correlated single photon counting system using a mode locked Nd-Yag laser and cavity damp dye laser with frequency doubling as excitation pulse source (λ = 300 nm, 1 ps full width at half maximum) as described by Huppert et al. (1990).

The emission of undissociated pyranine (ΦOH^*) was monitored at 435 nm at pH = 5.0. Numerical reconstruction of the fluorescence decay was carried out using N. Agmon's program (Pines et al., 1988; Huppert et al., 1990; Agmon and Szabo, 1990).

RESULTS

Binding of pyranine to Apomyoglobin

Addition of pyranine to Apomyoglobin solution causes a major change in the emission fluorescence spectrum of the dye. The emission of the undissociated form ΦOH^* ($\lambda_{max} \sim 440$ nm) increases from ~5% (with respect to ΦO^{*-} emission at $\lambda = 515$ nm) up to equal intensities (see Fig. 1). The emission enhancement was used by Gutman and Nachliel (1982) to quantitate the stoichiometry (1:1) and stability of the complex. In this study we measured the stability of the complex as a function of temperature in the range 15–48°C, where the apoprotein retains its native configuration (Griko, Privalov, and Venyaminov, 1988). The results fit a linear Vant-Hoff plot with $\Delta H^0 = 2.3 \pm 0.2$ Kcal/mol and $\Delta S^0 = -46.6$ eu ($n = 13$, $r = 0.995$).

The nature of the complex was investigated by studying the effect of ionic strength on the stability of the complex. The results, shown in Fig. 1, relate ΔG^0_{obs} vs. $\sqrt{I}$ in the range 0–80 mM NaCl.

For the purpose of the analysis ΔG^0_{obs} was taken as a sum of electrostatic interactions (ΔG^0_{el}) which is sensitive to the ionic strength, while all other terms are defined as ΔG^0_{other}. ΔG^0_{el} is the difference between the electrostatic energy of the dye-protein complex vs. that of the protein and the dye.

$$\Delta G^0_{el} = W_{el}(\text{complex}) - [W_{el}(\text{prot}) + W_{el}(\text{dye})] \quad (1)$$

For each species W_{el} is given by:

$$W_{el} = \frac{Z^2 e_0^2}{2\epsilon R}\left(1 + \frac{\kappa R}{1 + \kappa a}\right), \quad (2)$$

where R is the radius of the species (20 Å for the protein, (Adams, 1976; Hassinof and Chisti, 1982)). κ is the reciprocal of Debye's length; Z is the charge of the species; and $a = R + 1$.

The charge of the apoprotein at pH = 5, based on its amino acid composition, was estimated to be ~10. The charge of the dye is −3 and that of the complex is sum of both. To analyze our experimental data we treated both Z_{prot} and ΔG^0_{other} as adjustable parameters and looked for a combination which will reproduce the observed dependence of ΔG^0_{obs} on $\sqrt{I}$. The curve shown in Fig. 1 is a singular solution and corresponds with $Z_{prot} = +11$ and $\Delta G^0_{other} = 2.5 \pm 0.2$ Kcal/mol.

This solution indicates that the complex is mostly electrostatic in nature, yet hydrophobic interactions between the ring structure and the amino acids in the site also play a role in the placement of the dye.

The complex between the protein and dye was simulated by the FRODO program using the atomic coordinates of the holoprotein, omitting the heme moiety from the site. The pyranine could be easily fitted into the cavity in a way that the three sulfono moieties of the dye interact with the basic groups of His 93, His 97, and Arg 45. The distance between one of the sulfono oxygens and the basic nitrogen (for each pair) was 2.5–3.1 Å. Such distance is compatible with a stable salt bridge. This conclusion is corroborated by fluorescence anisothropic measurements that failed to detect any rapid rotation of the dye when complexed with the Apomyoglobin.

Dynamic measurement of a single proton within the heme binding site

Fig. 2 depicts a time resolved fluorescence of ΦOH^*. Curve *A* was recorded with the dye dissolved in water.

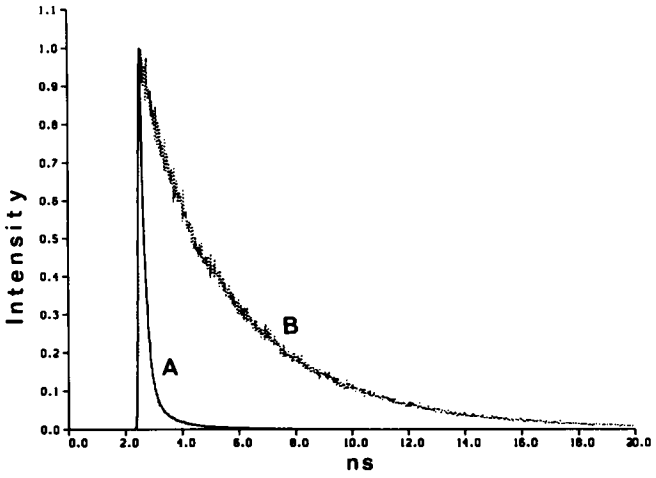

FIGURE 2 Time resolved fluorescence of pyranine at the wavelength of ΦOH* emission. Curve *A* was measured for the dye dissolved in water; curve *B* for the dye protein complex (measured at 5:1 excess of Apomyoglobin). The dynamics were measured with ~30 μM dye at pH 5.0.

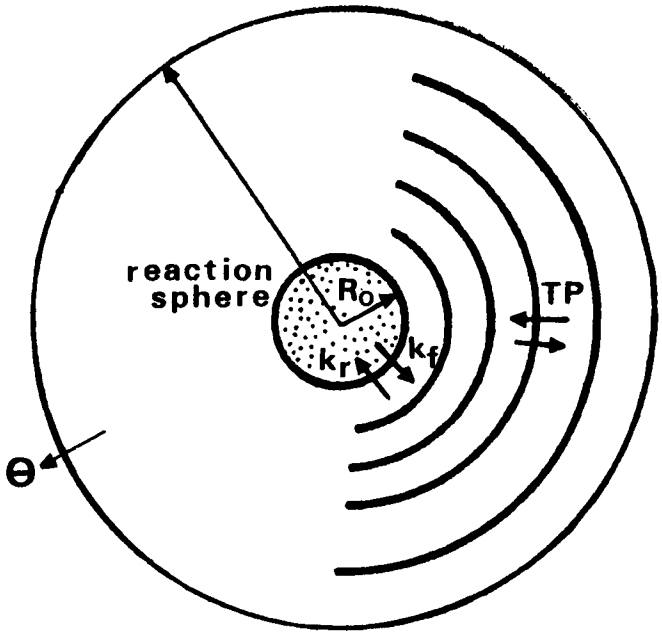

SCHEME 1

Initially the emission of ΦOH* decays with $\tau \sim 110$ ps, corresponding to the dissociation of H^+ and formation of ΦO^{*-}. About 0.5 ns after excitation the decay slows considerably to a long, nonexponential tail. That slow fading of emission is due to replenishment of ΦOH* population by the geminate recombination of H^+ and ΦO^{*-} (Huppert, Pines, and Agmon, 1990).

The same process within the heme binding site of the Apomyoglobin (curve *B*) exhibits a very slow, multiexponential decay curve (see Fig. 3). Apparently the proton and ΦO^{*-} in the cavity experiences repeated dissociation recombination events which persist repeatedly until the dye decays to ground state or H^+ escapes to the bulk.

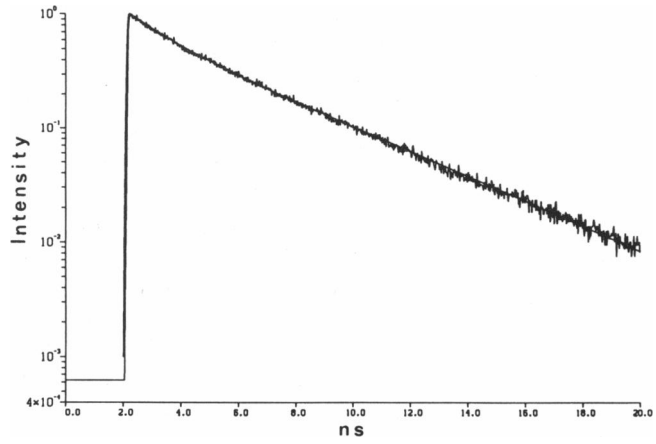

FIGURE 3 Theoretical reconstruction of the ΦOH* fluorescence emission dynamics of the pyranine Apomyoglobin complex. The curve was generated by N. Agmon's computer program (Pines et al., 1988) using the parameters listed in Table 1. The experimental curve is that shown in Fig. 2, (*trace B*), drawn on a logarithmic *Y* scale. The theoretical dynamics is given by the continuous line.

The reconstruction of the observed signal is based on the differential form of the Debye Smoluchowski equation for the time-dependent translational diffusion of a charged particle in a Coulombic potential field (Pines et al., 1988; Huppert et al., 1990). The reaction is described as taking place between radiating boundaries which are equated with the pyranine anion and the protein-water interface of the heme binding site (see Scheme 1). The inner boundary R_0 represents the pyranine. The rates of proton production and consumption at $r = R_0$ are defined by k_f and k_r, respectively.

Any proton approaching R_{max} has a certain probability of being absorbed (Θ), otherwise it is reflected inward. In contrast to the reaction at $r = R_0$, where repeated association–dissociation cycles can take place, at R_{max} the absorption of the proton is irreversible, indicating that a proton lost to the bulk will not diffuse back to the cavity within the lifetime of ΦO^{*-}. Between these boundaries the proton diffusion is treated by Agmon's program as diffusing between concentric shells. The probability for transition between adjacent shells $r(i)$ and $r(j)$ is given by the following expression:

$$TPi/j = \frac{D_{H^+}}{\Delta r^2} \cdot \frac{r_i}{r_j} \cdot \exp\left(-\frac{R_D}{2}\left(\frac{1}{r_i} - \frac{1}{r_j}\right)\right). \quad (3)$$

The first term in Eq. 3 defines through the diffusion coefficient, the frequency of the transition. The second term, the radii ratio of the respective shells, favors the transition away from the anion. It represents the tendency of diffusive processes to increase the entropy of the system. The last term in the equation defines the effect of the

TABLE 1 **The microscopic parameters that reconstruct the observed fluorescence dynamics of pyranine dissolved in water or in the heme binding site of Apomyoglobin**

Parameter	Apomyoglobin	H_2O
Radius of reaction (Å)	4 ± 0.25	6.5
R_{max} (Å)	10 ± 0.5	Not applicable
k_f (s^{-1})	$2.2 \pm 0.1 \times 10^8$	7.10^9
k_r (cm s^{-1})	$2.2 \pm 0.2 \times 10^8$	6.10^9
R_D (Å)	65 ± 2.5	28.3
ϵ_{obs}	8.4	78
D_H + cm^2 s^{-1}	$4 \pm 0.5 \times 10^{-5}$	9.3×10^{-5}
θ	10%	Not applicable

The magnitude of θ was estimated from the orientation of the heme in the protein (Adams, 1976).

gradient of the Coulombic potential on the transition probability, where R_D is the distance where the electric potential equals the thermal energy

$$R_D = Z_1 Z_2 e_0^2 / \epsilon kT. \quad (4)$$

For a detailed description of the mathematical operations see Pines et al. (1988), Huppert et al. (1990), Agmon and Szabo (1990), Gutman, Nachliel, and Kiryati (1992).

The program propagates the proton in space and time using the transition probabilities and the momentary probability density of protons ($P(r; t)$). The variation of $P(r = 0, t)$, namely the probability of finding a proton inside the reaction sphere, is the dynamics of the ΦOH* species and, when multiplied by its fluorescence decay function ($e^{-t/\tau}$) should replicate the observed fluorescence dynamics. In practice, to attain a reconstruction of the experimental tracings, the following parameters k_r, k_f, D_{H+}, and R_D were varied to obtain a fit as good as that shown in Fig. 3. The fitting of the curve is very much assisted by the fact that each parameter affects the dynamic in its peculiar way and cannot be mimicked by one or a combination of other parameters. Thus we regard the solution, as shown in Fig. 3, to be unique.

The parameters required for that reconstructed dynamics are given in Table 1.

DISCUSSION

In this study we investigated the properties of the Myoglobin's heme binding site after replacing the bulky heme group by a smaller dye molecule, pyranine, while the vacant space is taken up by water. The measurements were initiated by a short synchronizing light pulse and we monitored the relative motion of the proton with respect to the protein bound dye. The strong multiplex binding of the dye to the positive anchoring groups in the site ensure that its intracavity placement is invariable during the observation time, while neither rotational nor translational motion of the protein has any effect on the observed signal. This unique observation mode bears some inherent disadvantage, in that the space under study is not given to manipulation. Interference with the binding of the dye will change the equilibrium population of complexed dye, not the situation within the individual sites occupied by the dye.

The binding of pyranine to Apomyoglobin is basically an electrostatic interaction, where the three negative charges of the sulfono moieties interact with three positive charges at the heme binding pocket. This description is confirmed by the effect of ionic strength on the stability of the complex (Fig. 1). The calculations of ΔG^0 in this figure were based on the Debye-Huckle formalism for the transformation of the charged pyranine moiety ($Z = -3$) from bulk water into an uncharged state within the protein. It bears no information about the intensity of electrostatic interaction inside the cavity, as they come into play wherever a charge, like a proton, is generated within this closed space.

The inside of the cavity, where the pyranine is bound, differs markedly from the bulk phase. The differences emerge from the dielectric discontinuity between water and protein, the shape of the boundary, the impenetrability of protons through the matrix of the protein, the ordering of water by the protein and the dimension of the proton permeable space. All these peculiarities were considered during the theoretical reconstruction of the dynamics (see Scheme 1).

(a) The electrostatic interactions within the cavity

The dielectric constant of a homogenous matrix is a continuum property characterizing the polarity and polarizability of the molecules; it is equal in size at any point in space. Near a boundary ($\epsilon_1 \neq \epsilon_2$) the dielectric constant is a function of the polarity of both matrixes and its value varies both with the distance and the shape of the boundary. Gilson et al. (1985) calculated the electrostatic interaction between charges in a spheric space of a low dielectric matter surrounded by water. The same formalism is applicable for calculating the interaction between charges inside a spherical water space surrounded by a low dielectric matter, which is the essence of our case. (The finite size of the protein was not considered.)

The electrostatic potential of ion pair within our model space consists of two components: both are a function of the relative position of the charges. One is the Coulomb potential $G_{ij} = Q_i Q_j / \epsilon_{eff} r_{ij}$ and the other is the self energy $G_{ii} = Q_i^2 / 2\epsilon_{eff} r_{ii}$, where Q_i and Q_j are the charges, r_{ij} and r_{ii} are the distance between charges and their ionic radii, respectively. ϵ_{eff} is the effective dielectric constant which varies with position of each charge. The total potential of the pair G_{TOT} is the sum of the Coulombic potential and the self energy (Gilson et al., 1985; see the appendix).

The equations of Gilson et al. (1985) were adapted to calculate the electrostatic interactions between proton and pyranine anion bound in the heme binding site. The

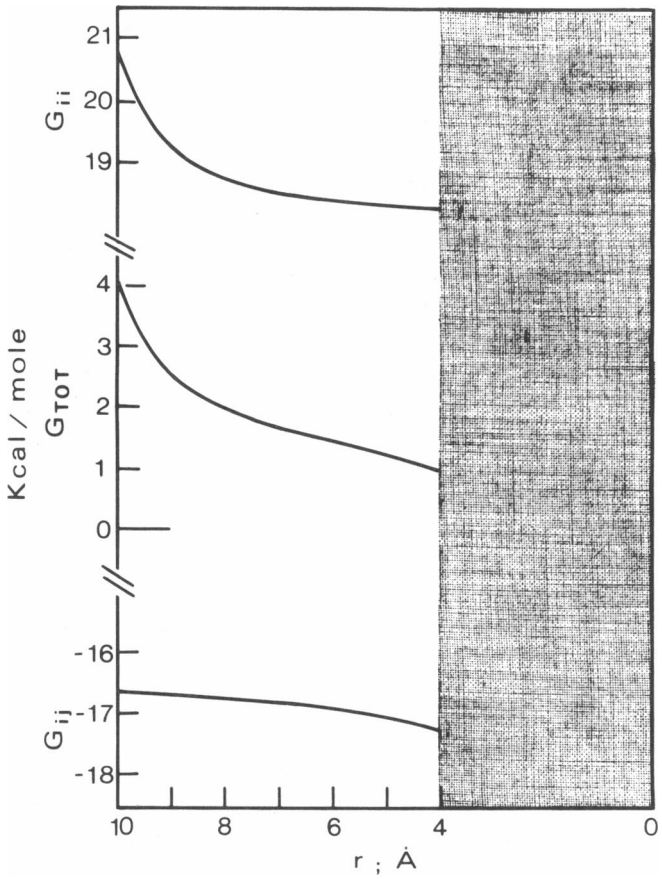

FIGURE 4 The electrostatic potential of an ion pair enclosed by an aqueous spheric cavity (r = 10 Å) surrounded by low dielectric matrix (ϵ = 2). The upper curve depicts the self energy (G_{ii}) of the cation (Z = +1, r_{ii} = 1.5 Å) as it varies with its radial position. The lower curve relates the pair potential G_{ij} with the radial position of the cation. The anion $Z = -1$, r_{jj} = 4 Å is located at the center of the cavity. The middle curve sums up the two potentials ($G_{TOT} = G_{ij} + G_{ii}$). Note the discontinuity of the ordinate. The potentials were not calculated inside the reaction sphere (*shaded area*) where the ions merge to a covalent bond.

potential of the ion pair was calculated for two configurations. In one, the pyranine was located at the center of the aqueous sphere, while in the other it was shifted to be in contact with the protein. The latter requires much more computations, yet the properties of space were (within 10%) similar to those calculated for a centrosymmetric one. Thus, for the sake of simplicity, we shall describe only the concentric model.

Fig. 4 depicts the variation of G_{ij} (*lower curve*), G_{ii} (*upper curve*), and G_{TOT} (*middle curve*) as they vary for a proton placed between R_0 and R_{max}. The shaded bar describes the inside of the reaction sphere where the proton loses its charge and exists as a covalently bound hydrogen.

The pair potential (G_{ij}) is lowest at contact radius and increases asymptotically to a constant value towards the edge of the cavity. The self energy term (G_{ii}) is constant at the central section of the cavity and increases steeply near R_{max}. The sum of the two (G_{TOT}) cancel much of the positive and negative bias, producing a funnel shaped potential curve, where the innermost position is favored by ~3 Kcal/mol (for ϵ_{prot} = 2). Over that electrostatic hill the proton must diffuse before coming to the sill from which it can step out to the bulk.

The shape and magnitude of the electrostatic barrier is drawn in Fig. 5 for different values of ϵ_{prot}. We see that very close to the reaction sphere the potential of the proton is almost indifferent to the dielectric constant, yet as the proton approaches the outer boundary, its potential becomes very sensitive to the polarizability of the protein.

The variation of ϵ_{eff} as a function of the radial coordinate is shown in Fig. 6. Within the proton permeable space, ϵ_{eff} falls from a high value at the edge of the reaction sphere down to that of ϵ_{prot} at contact with the protein.

The curves of ϵ_{eff} vs. r are instrumental for analyzing the experimental ϵ_{eff} and deducing what is ϵ_{prot}. For this we intregrated the value of $\epsilon_{eff}(r)$ over the whole reaction space and normalized it by its volume. This averaged parameter is equated with ϵ_{obs} (see Table 1)

$$\bar{\epsilon}_{eff} = \frac{\sum_{0}^{R_{max}} \epsilon_{eff}(r) \cdot 4\pi r^2}{\sum_{0}^{R_{max}} 4\pi r^2}. \quad (5)$$

The dependence of $\bar{\epsilon}_{eff}$ on ϵ_{prot} is shown in Fig. 7. The experimentally measured value ϵ_{obs} = 8.4 corresponds with a dielectric constant $\epsilon_{prot} \leq 6.5$.

The dielectric constant of microscopic structures was measured in other systems too. The pore of the anion specific porin Pho.E, is characterized by ϵ = 24 (Tsfadia, 1991). The intermembranal space between egg PC multilamellar was determined to be ϵ = 40 (Gutman, Nachliel, and Kiryati, 1992b), and the α amine region of lyso-

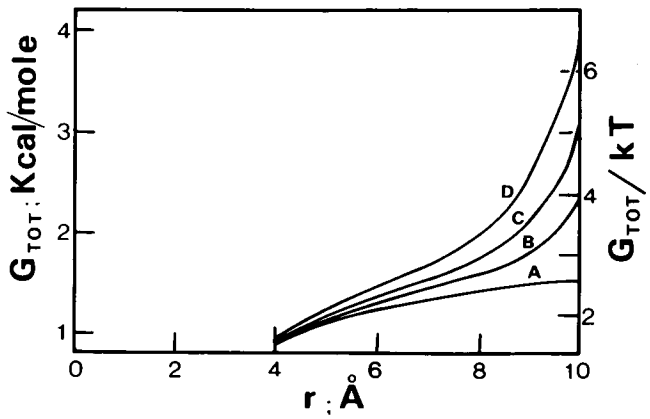

FIGURE 5 The radial dependence on the dielectric constant of a proton and centrosymmetric anion in a small aqueous sphere (r = 10 Å) on the dielectric constant of the surrounding matrix. Curve A was calculated for ϵ_{prot} = 78, i.e., ion pair in bulk water. The dielectric constant corresponding with the other curves decreases to ϵ_{prot} = 40 (B), 20 (C), and 2 (D).

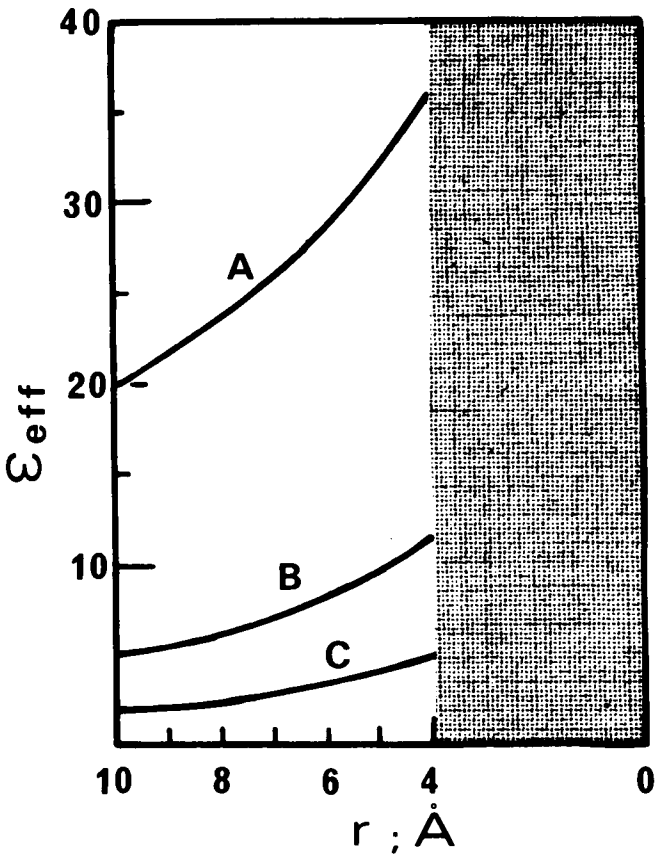

FIGURE 6 The radial variation of the effective dielectric constant calculated for an aqueous sphere (r = 10 Å) surrounded by envelope with ϵ = 20 (*upper curve*) ϵ = 5 and ϵ = 2 (*middle* and *lower curve*, respectively). The dielectric constant inside the reaction sphere (r = 4) was not calculated.

zyme has ϵ = 13.5 (Yam et al., 1991). Thus the effective dielectric constant of a small cavity varies with its shape and the nature of the low dielectric boundary.

(b) The water in the cavity

There are two indices in our study which are related with the properties of the water inside the site; the rate of proton dissociation (k_f) and the diffusion coefficient of the proton (D_{H+}). Both of them indicate that the few water molecules in the cavity (less than 30) exhibit a slower rate of rotation.

The rate of proton dissociation in aqueous systems is a function of the activity of water surrounding the dissociating molecule (Huppert et al., 1982). For many compounds the dependence is a linear logarithmic function with a slope depending on the dissociating species (Gutman, 1984).

The lowered activity is associated with limited capacity of the water molecule to stabilize (by hydration) the dissociating proton within the time frame of the O—H vibration. The slower rate of proton dissociation (k_f = $2.2 \cdot 10^8$ s^{-1}) measured in the heme binding site corresponds with a_{H_2O} = 0.61 (see Gutman and Nachliel, 1982).

The diffusion of proton in water proceeds by an exchange of H^+ between two hydrogen bonded water molecules ($H_3O^+ — H_2O$) at a frequency of $\sim 2 \cdot 10^{13}$ s^{-1}. Exchange of proton between water molecules must be supplemented by random element to become a diffusion. The randomicity is provided by a much slower process, the formation and dissolution of hydrogen bonds between water molecules, a process with a time constant of $\tau \sim 2.3$ ps.

The combination of the frequency of the random stepping ν and the length of the step (L) determines the diffusion coefficient $D = \nu L^2/2$. As we assume that the length of the random step cannot be shorter than the distance between water molecules, the smaller value of D_{H+}, as measured in the heme binding site, indicates that the frequency of stepping is reduced, i.e., enhancement of the order parameter of water.

(c) The dynamics of a free proton in a microscopic cavity

The rate at which a proton propagates within a microscopic cavity is basic information required for understanding the mechanism of all proton coupled bioenergetic processes. This study is the first glance at the dynamics of a single proton inside a cavity in a protein. The theoretical treatment which reconstructs the fluorescence of the pyranine in the site can also reconstruct the spatio-temporal distribution of proton in the site (see Fig. 8). The vertical axis in this figure denotes the probability of finding a proton at a given radial position (*right side abcissa*) and time (*left side abcissa*).

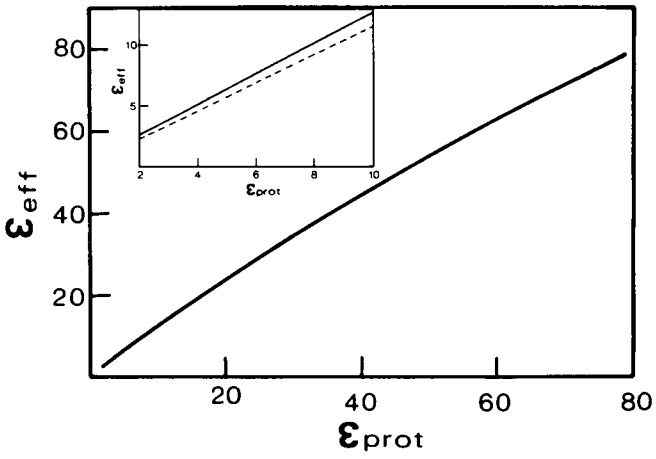

FIGURE 7 The dependence of the averaged effective dielectric constant ($\bar{\epsilon}_{eff}$) of an aqueous sphere (r = 10 Å) on the dielectric constant of the surrounding matrix. $\bar{\epsilon}_{eff}$ was calculated according to Eq. 5 for a centrosymmetric configuration. (*Inset*) An enlargement of the lower section of the main frame, using centrosymetric configuration (----) or an off-center placement of the anion to be in contact with the edge of the aqueous sphere (– –).

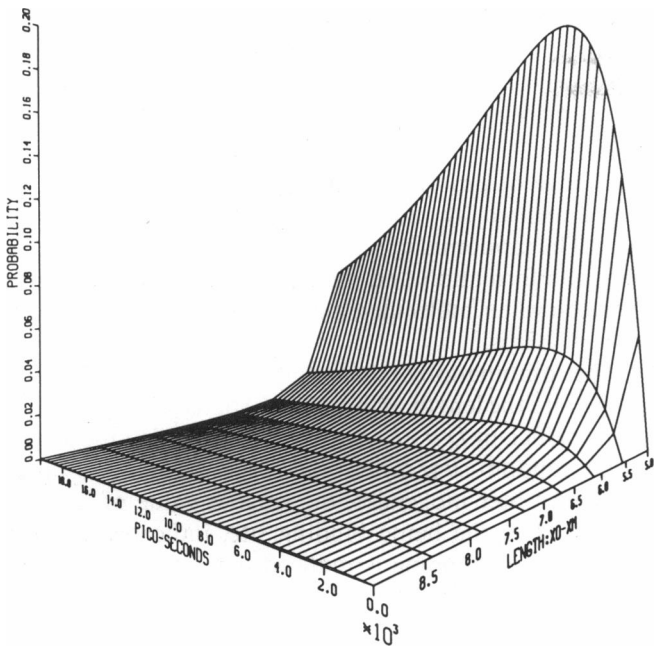

FIGURE 8 Spatio-temporal mapping of the proton probability inside the aqueous cavity representing the heme binding site of Apomyoglobin. The cavity is 10 Å in radius, having the experimental value of ϵ_{eff} and 10% absorption at r = 10 Å. The other parameters are those in Table 1. The vertical axis represents the probability of finding a proton at distance r (given on the *right side abscissa*) and time (marked on the *left side abscissa*).

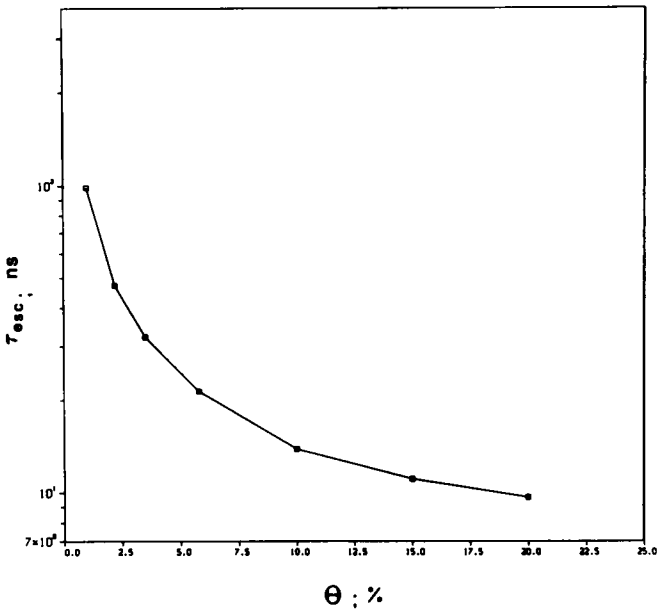

FIGURE 9 The dependence of the proton's escape time on the relative size of the orifice connecting a small cavity (r = 10 Å) with the bulk phase. The calculations were carried out for the model fitting best the Apomyoglobin cavity (see Fig. 3) while varying the ratio between the surface of orifice to surface of sphere (given in percentage of the abscissa). The escape time was calculated from the almost exponential decay of the population of free protons remaining in the cavity.

Within the first ~3 ns the discharged proton probes the whole volume of the reaction space and the radial probability is stabilized to follow the potential field. From that time on, the proton density within the cavity decays without major changes in the radial distribution pattern. Both processes, probing the site ($\tau \sim 3$ ns) and the leakage ($\tau \sim 14$ ns) are fast reactions. Their time scale is orders of magnitude faster than the turnover time of bioenergetic enzymes (~1 ms).

Two parameters can delay the proton in the cavity, narrow opening which slows the emergence of protons to the bulk and electrostatic potential which attracts the proton to the interior of the cavity, the Mitchellian "proton well". The role of the two terms can be evaluated by numerical simulation, using the heme binding site as a model. In one set of computations we varied θ (see Scheme 1) and investigated how it affects the escape time. In the other, the energy barrier detailed in Fig. 5 was the variable. Fig. 9 depicts the effect of the orifice size on the escape time of the proton. As seen in this figure, the site becomes effectively confining only when the opening to the bulk is extremely small. To delay a proton for more than 1 microsecond the orifice must be smaller than the size of a water molecule.

The effect of the electrostatic potential on the dwell of a free proton is shown in Fig. 10, where the escape time is related with the height of the potential barrier between R_0 and R_{max} (given in kT units). We find that prolonged confinement of a proton to τ_{esc} = 400 ns, calls for ΔG = 15 kT, a value almost 50% higher than maximal $\Delta\psi$ measured in well coupled biomembranes. Thus, neither elec-

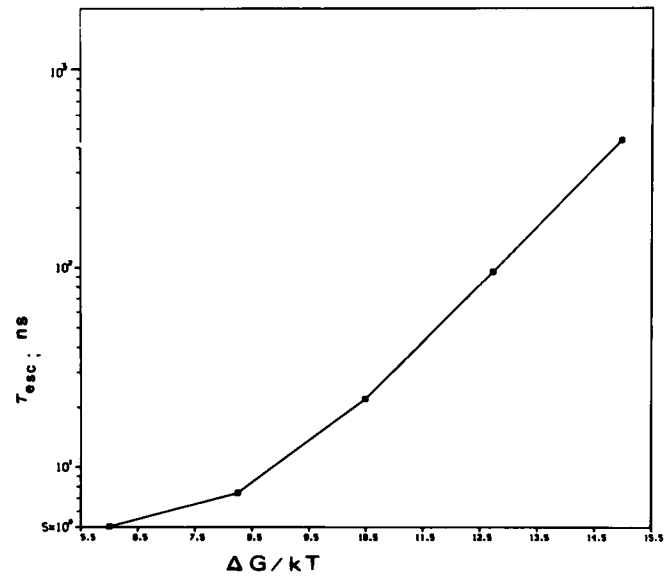

FIGURE 10 The effect of electrostatic potential on the escape time of a proton from a small aqueous cavity. The calculations were carried out for the best fitting model of the Apomyoglobin site (see Fig. 3). The electrostatic potential, drawn on the abscissa in kT units, is the difference between the proton potential at r = 4 and r = 10 (see Fig. 5).

trostatic barriers nor narrow openings can delay the elusive free proton for a period comparable to the turnover time of energy conserving enzymes. The delay of proton(s) within an active site necessitates their storage as covalently bound hydrogen atoms, attached to suitable moities within the protein.

CONCLUDING REMARKS

In this study we exploited our advantage to monitor, in a time-resolved mode, the dynamics of a single proton in a well defined microscopic cavity. The experimental observations are supported by a powerful analytic procedure which reconstructs theoretically the observed signal. This mode of analysis provides unambiguous quantitation of the dielectric constant and the proton diffusion coefficient which characterizes the probed space. Both parameters are amendable for further interpretation.

The diffusion coefficient indicates that the lifetime of the hydrogen bonds between water molecules, close to the protein's surface, is longer than in the bulk.

The dielectric constant of a small cavity is a function of shape and size. Knowing these parameters allowed us to determine the dielectric constant of the protein itself. For this case we estimate the dielectric constant of the protein to be, $\epsilon_{Prot} \leq 6.5$.

The capacity to measure and analyze the dielectric properties of mesoscopic structures, such as an active site of a protein, will lead to further understanding of the electrostatic forces and contribute to the correlation between structure and function using defined physical terminology.

This research is supported by the American Israeli Binational Science Foundation (87 0035) and the Office of Naval Research (United States Navy grant N00014-89-J1622).

Received for publication 1 October 1991 and in final form 28 July 1992.

REFERENCES

Adams, A. P. 1976. The kinetics and mechanism of the recombination reaction between Apomyoglobin and hemin. *Biochem. J.* 159:371–376.

Agmon, N., and A. Szabo. 1990. Theory of reversible diffusion-influenced reactions. *J. Chem. Phys.* 92:5270–5284.

Antonini, E., and M. Brunori. 1971. Hemoglobin and myoglobin and their reactions with ligands. *Frontiers Biol.* 21:123–125.

Cao, Y., G. Varo, R. Needleman, M. Chang, B. Ni, and J. Lanyi. Bound water is required for proton transfer from aspartate 96 to the bacteriorhodopsin Schiff base. *Biochemistry.* In press.

Gerwert, K., G. Souvignier, and B. Hess. 1990. Simultaneous monitoring of light-induced changes in protein side-group protonation, chromophore isomerization, and backbone motion of bacteriorhodopsin by time-resolved Fourier-transform infrared spectroscopy. *Proc. Natl. Acad. Sci. USA.* 87:9774–9778.

Gilson, M. K., A. Rashin, R. Fine, and B. Honig. 1985. On the calculation of electrostatic interactions in proteins. *J. Mol. Biol.* 183:503–516.

Griko, Y. V., P. L. Privalov, and S. Y. Venyaminov. 1988. Thermodynamic study of the Apomyoglobin structure. *J. Mol. Biol.* 202:127–138.

Gutman, M., and E. Nachliel. 1982. Direct measurement of proton transfer as a probing reaction of the Apomyoglobin heme binding site. *Eur. J. Biochem.* 125:175–181.

Gutman, M. 1984. The pH jump: probing of macromolecules and solutions by a laser-induced, ultrashort proton pulse theory and applications in biochemistry. *Methods Biochem. Anal.* 30:1–103.

Gutman, M., E. Nachliel, and S. Kiryati. 1992a. Dynamic studies of proton diffusion in mesoscopic heterogeneous Matrix. I. Concentrated solutions of sucrose. *Biophys. J.* 63:274–280.

Gutman, M., E. Nachliel, and S. Kiryati. 1992b. Dynamic studies of proton diffusion in mesoscopic heterogeneous Matrix. II. Intermembranal space between phospholipid membrane. *Biophys. J.* 63:281–290.

Hasinoff, B. B., and S. B. Chishti. 1982. Viscosity dependence of the kinetics of the diffusion-controlled reaction of carbon monoxide and myoglobin. *Biochemistry.* 21:4275–4278.

Henderson, R., J. M. Baldwin, T. A. Ceska, F. Zemlin, F. Beckmann, and K. H. Downing. 1990. Model for the structure of bacteriorhodopsin based on high-resolution electron cryomicroscopy. *J. Mol. Biol.* 213:899–929.

Huppert, D., E. Kolodney, M. Gutman, and E. Nachliel. 1982. Effect of water activity on the rate of proton dissociation. *J. Am. Chem. Soc.* 104:6949–6953.

Huppert, D., E. Pines, and N. Agmon. 1990. Long time behavior of reversible geminate recombination reactions. *J. Opt. Soc. Am. B.* 13:1545–1550.

Kornblatt, J. A., and G. Hui Bon Hoa. 1990. A nontraditional role for water in the cytochrome oxidase reaction. *Biochemistry.* 29:9370–9376.

Matthew, J. B., and F. M. Richards. 1982. Anion binding and pH dependent electrostatic effects in ribonuclease. *Biochemistry.* 21:4989–4994.

Pines, E., D. Huppert, and N. Agmon. 1988. Geminate recombination in the excited state proton transfer reaction: numerical solution of the Debye-Smoluchowski equation with back reaction and comparison with experimental results. *J. Chem. Phys.* 88:5620–5630.

Shimoni, E., E. Nachliel, and M. Gutman. 1993. Gaugement of the inner space of the Apomyoglobin's heme binding site by a single free diffusing proton. II. Interaction with bulk proton. *Biophys. J.* 64:480–483.

Varo, G., and J. K. Lanyi. 1990. Pathways of the rise and decay of the M photointermediate(s) of bacteriorhodopsin. *Biochemistry.* 29:2241–2250.

Varo, G., and J. K. Lanyi. 1991. Kinetic and spectroscopic evidence for an irreversible step between deprontonation and reprotonation of the Schiff base in the bacteriorhodopsin photocycle. *Biochemistry.* 30:5008–5015.

Yam, R., E. Nachliel, S. Kiryati, M. Gutman, and D. Huppert. 1991. Proton transfer dynamics in the nonhomogeneous electric field of a protein. *Biophys. J.* 59:4–11.

Zimmerburg, J., and V. A. Parsegian. 1986. Polymer inaccessible volume changes during opening and closing of voltage dependent ionic channels. *Nature (Lond.).* 323:36–39.